Crimson Publishers
Wings to the Research

Research Article

Modeling Sources of Fracture Toughness for an Intercalated Nanoclay/Epoxy

Marouf BT[1]*, Pearson RA[2] and Bagheri R[3]

[1]Department of Materials Science and Engineering, Faculty of Engineering, Iran

[2]Center for Polymer Science and Engineering, Department of Materials Science and Engineering, USA

[3]Polymeric Materials Research Group, Department of Materials Science and Engineering, Iran

ISSN: 2770-6613

***Corresponding author:** BT Marouf, Department of Materials Science and Engineering, Faculty of Engineering, Urmia University, Urmia, Iran

Submission: October07, 2020
Published: December 14, 2020

Volume 1 - Issue 3

How to cite this article: Marouf BT, Pearson RA, Bagheri R. Modeling Sources of Fracture Toughness for an Intercalated Nanoclay/Epoxy. Polymer Sci Peer Rev J. 1(3). PSPRJ. 000513. 2020.
DOI: 10.31031/PSPRJ.2020.01.000513

Abstract

The novelty of this paper is to quantify the contribution of micro mechanisms caused the changes in fracture behavior of a model system epoxy resin by introduction of intercalated nano clay. To achieve this aim, a combination of fracture toughness measurements, electron and optical microscopy assessments and analytical models have been used. The results obtained indicated that addition of intercalated nano clay increased fracture toughness of the epoxy resin, although the increases in toughness were modest. Examination of fracture surfaces and subsurface damage revealed the presence of crack deflection, particle bridging and crack branching/microcracking mechanisms. Analysis of the micromechanical models for these toughening mechanisms suggested that crack branching contributes the most to the increase in toughness. In addition in the present study, the possible additive effects of crack path deflection, crack wake bridging, and crack branching and microcracking have been observed as the sources of modest improvements in toughness for these intercalated clay-filled epoxies.

Keywords: Modeling; Toughening mechanism; Intercalation;Nano clay; Epoxy

Abbreviations: TEM: Transmission Electron Microscope; DSC: Differential Scanning Calorimetry; SEM: Scanning Electron Microscope; TOM: Transmission Optical Microscopy

Introduction

Much research has been done to reinforce thermoplastic and thermosetting polymers with organic and inorganic particles [1-5]. For epoxy resins, it is known that micron-size particles are able to enhance mechanical properties [6-8]. However, the addition of micron-size fillers may not always improve the overall performance of a material, and in particular, improvements of some properties may occur to the expense of others properties [6,9]. Nano-size fillers have been under development to overcome these disadvantages. Nano clay is an inexpensive nanofiller with a great potential for usage in wide variety of applications. Numerous papers agree well on stiffening effect of nano clay in polymers [10-13] and many studies have been done to estimate increases in modulus of nano clay-filled polymers, nano clay/epoxies included [12,14-17]. Some research also has studied strengthening effect of nano clay in polymers using prediction models [12,18,19]. Based on the strengthening models, the importance of adhesion between nano clay layers has been demonstrated [12]. Furthermore, due to the importance of fracture toughness in epoxy resins, several scientific papers have focused on the fracture behavior of clay-epoxy nanocomposites [20-23]. According to the open existing literature on nano clay/epoxies, the increases in fracture toughness of these nano-materials have been attributed to different micro mechanisms such as matrix plastic deformation, crack deflection, crack bridging, or microcracking and there is no agreement on one active mechanism [22,24-27]. Marouf et al. [7] conclusively reviewed the existing literature on toughening effect of nano clay in epoxies and the potential mechanisms involved. In complement to the existing literature findings for better understanding of toughening mechanisms activated in nano clay/epoxy nanocomposites, the objective of this research is to quantify the contribution of possible sources involved in toughness improvement in a toughenable epoxy filled with intercalated nano clay using micromechanical models in combination with experimental results.

Experimental

Materials

In this investigation, clay-epoxy nanocomposites were synthesized by swelling an organophilic montmorilonite in an aromatic epoxy resin and subsequent polymerization. The epoxy resin used was a diglycidyl ether of bisphenol A (DGEBA), EPON 828, from Hexion Specialty Chemicals (USA). The epoxide equivalent weight of the epoxy resin is 184-190gmol^{-1}. The epoxy resin was used in combination with a curing agent, piperidine from Sigma-Aldrich (USA). The organoclay from Zhejiang Fenghong Clay (China) with the trade name of NANOLIN DK1 was used in this study while its concentration was varied systematically up to 15 wt%.

Nanocomposite preparation

For preparation of nanocomposites, organoclay powder was mixed with the appropriate amount of liquid epoxy resin using a Heidolph RZR2102 mechanical stirrer for 8h at 80 °C. Then, 5 parts curing agent per hundred parts resin (phr) was injected gently into the liquid suspension and mixed for 15min at the same temperature. Vacuum was then applied with stirring continued for another 15min to degas the mixture. Next, the mixture was cast into a preheated aluminum mold and cured at 120 °C for 16h to produce test specimens used to evaluate mechanical properties.

Characterization techniques

The nano-filler dispersion in the epoxy matrix was investigated using wide angle X-ray diffraction (WAXD). A Philips PRO Xpert with Cu-Kα radiation was used in this experiment. Dispersions of organoclay in the epoxy matrix was investigated by a transmission electron microscope (TEM). Samples were cut using a Leica Ultra cut UCT ultra-microtome with a diamond knife. Thin sections (60-80nm) were collected on copper grids and examined using a Philips CM200, field emission gun (FEG) TEM at an accelerating voltage of 200kV in bright field mode. Glass transition temperatures (Tg) of cured materials were measured using differential scanning calorimetry (DSC) in standard mode, TA Instruments 2920 Modulated DSC, at a heating rate of 10 °C min^{-1} in the range of 25-150 °C. The glass transition temperature was determined on the second heating cycle. Fracture toughness measurements were conducted on pre-cracked, single edge notched (SEN) specimens (72Î12.7∈5.8 mm) in three point bending (3PB) geometry and in accordance with the ASTM D5045. Pre-cracking was performed by tapping a chilled razor blade into the notch sawed in the specimens. These tests were conducted on a Hounsfield H10KS testing frame with a cross head speed of 1mm min^{-1}. The fracture toughness values represent averages of six tests and were obtained under plane strain condition. The following equations (1,2) were used to calculate K_{IC}:

$$K_{IC} = \frac{10^{1.5} \times P \times S}{t \times w^{1.5}} f(X) \quad (1)$$

and

$$f(X) = 3X^{0.5} \frac{\left[1.99 - X(1-X)(2.15 - 3.93X + 2.7X^2)\right]}{2(1+2X)(1-X)^{1.5}} \quad (2)$$

$$X = \frac{a}{w} \quad (3)$$

where P is the critical load for crack propagation, S is the span length, t is the specimen thickness, w is the specimen width, a is the crack length, f(X) is non-dimensional shape factor, and X is the ratio of the crack length to the specimen width.

A Cam Scan MV 2300, scanning electron microscope (SEM) was used to examine the fracture surfaces of the materials tested. All fracture surfaces were coated by a thin layer of gold prior to fractography to protect surfaces from beam damage and charge buildup. In order to observe the crack tip damage zone of the nanocomposites, the double notched four-point bending (DN-4PB) method in conjunction with transmission optical microscopy was employed. Specimens, 5.8 millimeter-thick, were used for this study. The screw-driven Hounsfield was also used at a crosshead speed of 1mm min^{-1} for breaking the samples. Thin specimens taken from the mid-plane of samples (plane strain region) were then viewed using an Olympus BH transmission-light microscope. Both bright field and crossed-polarized light conditions were employed.

Results and Discussion

The result of XRD and TEM studies in order to evaluate the dispersion state of organoclays in the epoxy matrix are illustrated in Figure 1. These studies show swelling of galleries and successful penetration of the clay galleries with pre-polymer which suggests the intercalation of organoclay in the epoxy matrix. The spacing between platelets was increased to about 3.5nm. More details on the XRD and TEM examinations are fully presented in part 1 of this study [12]. The glass transition temperature of epoxy compounds was investigated using DSC. The DSC results reported in Table 1 indicate that the materials are fully cured and that clay surfactants do not interfere with the curing reaction. Also, since Tg is substantially unchanged, this proposes that the epoxy is not tightly bound to filler [28]. This agrees well with the strengthening results reported by the same researchers [12]. In summary, no change in the glass transition temperature of the epoxy resin was observed as organoclay was added into the resin. (Figure 2) contains a plot of the fracture toughness, obtained by SEN-3PB tests, versus nano clay content. The KIC values are a function of nano clay loading and are modestly higher than that of the neat epoxy (Figure 3). This agrees well with the results reported in the literature [7,24,26,27,29-33]. The fracture toughness of the neat epoxy is 0.8MPam0.5. The 5 wt.% intercalated nano clay-filled epoxy exhibits the highest toughness at 1.19MPam0.5 so a 50% increase is observed. The fracture toughness of the nano clay-filled nanocomposite decreases slightly at 10 wt%. Poor dispersion of the nano clay particles at higher contents of 10 and 15 wt% could be the reason for lower fracture toughness compared to that of 5 wt% composite (Figure 4). Figure 3 illustrates the SEM micrographs taken from the damage zone on fracture surfaces of the nanocomposite containing 3 wt% organoclay. Compared to the neat epoxy, the fracture surface of the 3 wt% organoclay-epoxy is much rougher. The fracture surface of the neat epoxy is very smooth (not shown) which is typical for brittle

polymers and indicates a very low fracture resistance. As seen in the micrograph (Figure 3), the damage zone is much rougher than two other zones and crack propagated through different planes, which suggests crack deflection. Furthermore, there is evidence of formation of microcracks in the damage zone. The SEM micrograph at higher magnification also indicates pull out or bridging of clay stacks. Therefore, nano clay bridging may also contribute to the increase in toughness observed.

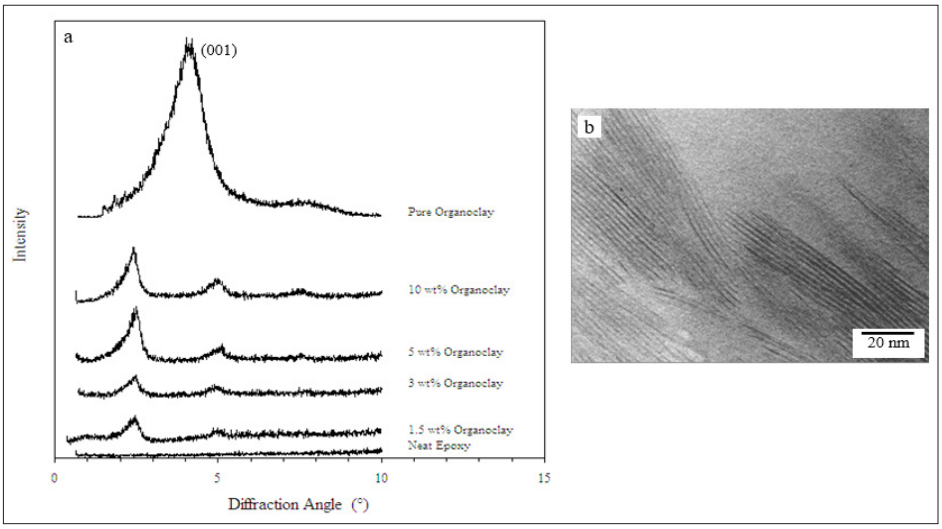

Figure 1: (a) X-ray patterns of pure organoclay, neat epoxy, and organoclay-filled epoxies. The shift in peak position from 4.2° to lower angles indicates increases in d-spacing between clay layers. (b) TEM micrographs of the 5 wt% organoclay-filled epoxy.

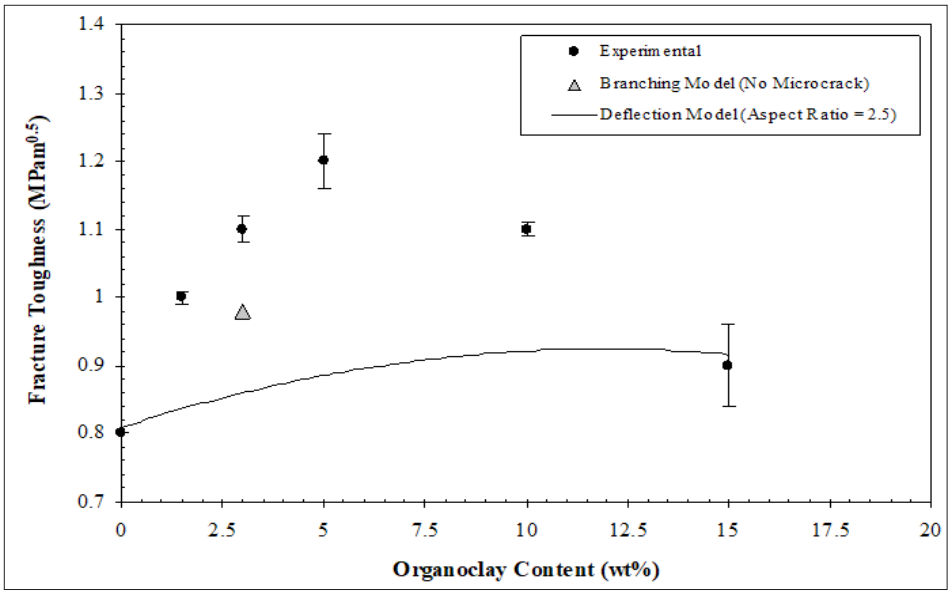

Figure 2: Fracture toughness (KIC) increases with nanoclay content up to 5 wt% in the epoxy matrix.

Table 1: Glass transition temperature of intercalated clay-filled epoxies measured using DSC.

Organoclay Content (wt%)	Tg (°C)
0	87
1.5	88.5
3	88
5	89
10	89
15	88

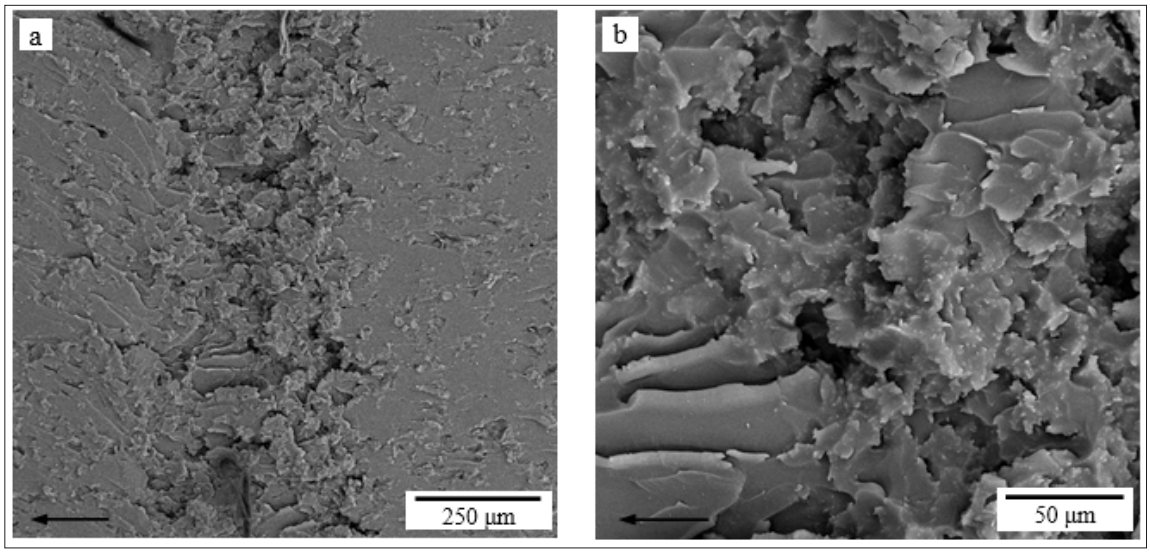

Figure 3: SEM micrographs showing the fracture surfaces of the 3 wt% clay-filled epoxy at two magnifications (a,b). The arrow shows the crack growth direction.

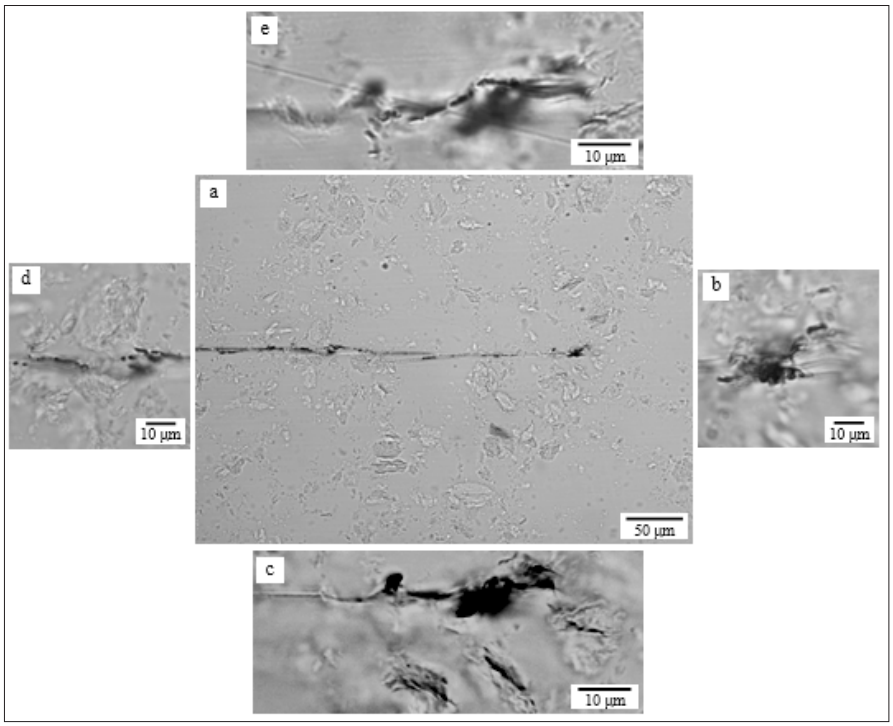

Figure 4: TOM micrographs taken near the crack tip in the 3 wt% clay-filled epoxy viewed under bright field: (a) lower magnification and (b-e) higher magnifications. Note the presence of crack path deflection in (a, c, and e), crack branching in (b), microcracking the tactoids in (c) and crack bridging in (d and e).

In general, transmission optical microscopy studies corroborate the SEM results. Figure 4 shows the TOM micrographs taken from the mid-plane near the crack tip of the 3 wt% intercalated clay-filled epoxy taken under bright field conditions. The path of crack propagation has been deflected in the nanocomposite (Figure 4a) while the crack has propagated in straight trajectory in the neat epoxy (not shown). In addition to crack wake deflections, the crack tip has branched out, and microcracking within the tactoids is found (Figures 4b & Figure 4c). It may be argued that microcracking the tactoids is an artifact formed during petrographic polishing, however, no sign of microcracks in clay tactoids is seen away from the crack tip. The TOM micrograph of nanoclay-filled epoxy clearly shows the breakage of organoclay tactoids (Figure 4d) and signs of bridging on the crack wake (Figure 4e). In summary, both SEM

and TOM, show that the improvement in toughness can be due to crack path deflection, second phase bridging, crack branching, and microcracking, which are well-known shielding mechanisms. In following paragraphs, an attempt is made to quantify the contribution of each of these mechanisms to the overall fracture toughness of these intercalated clay-filled epoxies. Several models have been developed to estimate the effect of crack path deflection on the overall fracture toughness [34,35]. Faber & Evans [35] proposed the following model to quantify the effect of crack path deflection as a source of improvement in fracture toughness as a function of Young's moduli ratio, volume fraction and aspect ratio of disk shape filler.

$$\frac{K_c}{K_m} = \left[\frac{E_c}{E_m}\left(1 + 0.57\varphi_f\left(\frac{r}{t}\right)\right)\right]^{0.5} \quad (3)$$

where Kc and Km are the fracture toughness of the filled material and the unfilled/neat material, respectively. E_c and E_m are the Young's moduli of the filled material and the unfilled/neat material, respectively and φ_f is the volume fraction of filler. r and t are radius and thickness of the disk shape filler. Please note that the aspect ratio of disk shape particle is equal to 2r/t.

Table 2: Fracture toughness prediction by deflection model proposed by Faber & Evans [35].

Organoclay Content		K_C/K_m				
E_C/E_m		Experimental	Prediction			
wt%	vol%	-	-	Aspect Ratio = 2.5	Aspect Ratio = 5	Aspect Ratio = 10
0	0	1	1	1	1	1
1.5	0.8	1.07	1.25	1.04	1.04	1.05
3	1.7	1.14	1.38	1.07	1.08	1.09
5	2.8	1.31	1.5	1.16	1.17	1.19
10	5.6	1.17	1.38	1.1	1.12	1.16

Aspect ratio = 2r/t.

Given that the ratio of Young's moduli from the experimental results and that the volume fraction of organoclay used and the aspect ratio of 2.5 (Table 2), it predicts only a 7% improvement in fracture toughness when this mechanism is operating in these organoclay-filled epoxies, while based on the experimental results, a 37% increase in fracture toughness was measured when 5 wt% (2.8 vol%) organoclay was added into the epoxy resin. For the 5 wt% organoclay-epoxy system, the model proposed by Faber & Evans [35] estimates only about 15% increase in toughness compared to a 50% improvement in the experimental result. In addition, as seen, the toughening effect is not a strong function of the aspect ratio of filler at the applied range. Comparing the predicted values and experimental results (Figure 2) reveals that although crack path deflection contributes to the overall toughening effect in intercalated clay-epoxies, but this cannot be the major source of toughening in these materials and other mechanisms should contribute to achieve a modest improvement in crack propagation resistance of organoclay-filled epoxies. Please note that morphological aspects such as particle size and aspect ratio are considered in the crack path deflection model proposed by Faber & Evans [35], although this model does not take account for the effect of agglomeration. Another possible toughening mechanism is crack branching and microcracking. Several types of microcracking mechanisms have been identified including particulate, matrix, and interfacial microcracks. (Figure 5) schematically illustrates three types of microcracks. Note that crack branching is a form of microcracking as well. In addition, several micro mechanisms models have been developed to estimate the contribution of microcracking to the overall toughness [36-40]. The following equation was developed by Gao & Wang [37] to estimate the toughening effect of crack branching and microcracking in ceramic materials, since in addition to microcracking; the main crack often exhibits branching:

$$\frac{K_c}{K_m} = \frac{1}{1 - \frac{\pi}{2}\left[\frac{\rho}{(3-\pi\rho)}\right]^{0.5}}\left[\left[2\cos\left(\frac{\beta}{2}\right)\right]\frac{\log 2}{\log\left[2\cos\left(\frac{\beta}{2}\right)\right]^{-1}} - \frac{p}{a}\left(\frac{\rho}{1-\pi\frac{\rho}{2}}\right)\right]^{0.5} \quad (4)$$

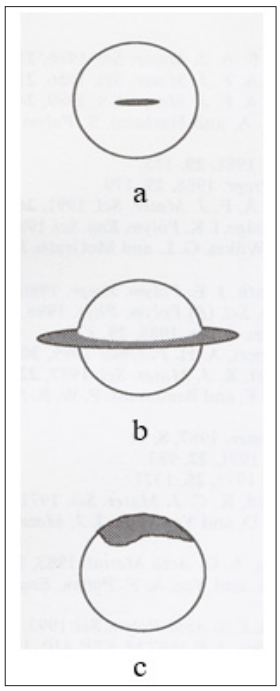

Figure 5: Schematics of three types of microcracks: (a) particulate, (b) matrix, and (c) interfacial [41].

where K_c is the fracture toughness of a material containing microcracks, K_m is the fracture toughness of a material without microcracks, β is the angle of the branched crack, 2a is the length of microcracks, ρ is the density of microcracks (number of microcracks per unit volume) and p is the width of the process zone. The schematic diagrams of microcracking model proposed by Gao & Wang [37] is seen in Figure 6.

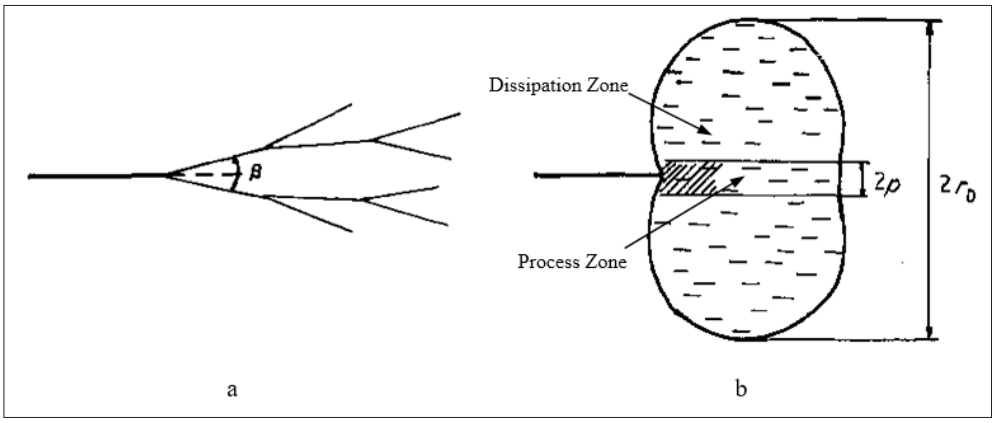

Figure 6: Schematic diagrams of microcracking model proposed by Gao & Wang [37]: (a) the model of the branched crack and (b) main crack tip showing "dissipation zone" and process zone.

This model predicts a logarithmic increase in fracture toughness by increasing the branching angle and a linear relationship between fracture toughness of the modified material and the density of the microcracks. Even though the model proposed by Gao & Wang [37] was developed from limited experimental results on a ceramic material, quantitatively this model gave a reasonable toughening prediction for a thermoplastic-modified epoxy [41]. Although it is difficult to precisely quantify the contribution of branching and microcracking to overall toughness, Gao & Wang's model [37] can assist in obtaining a rough approximation.

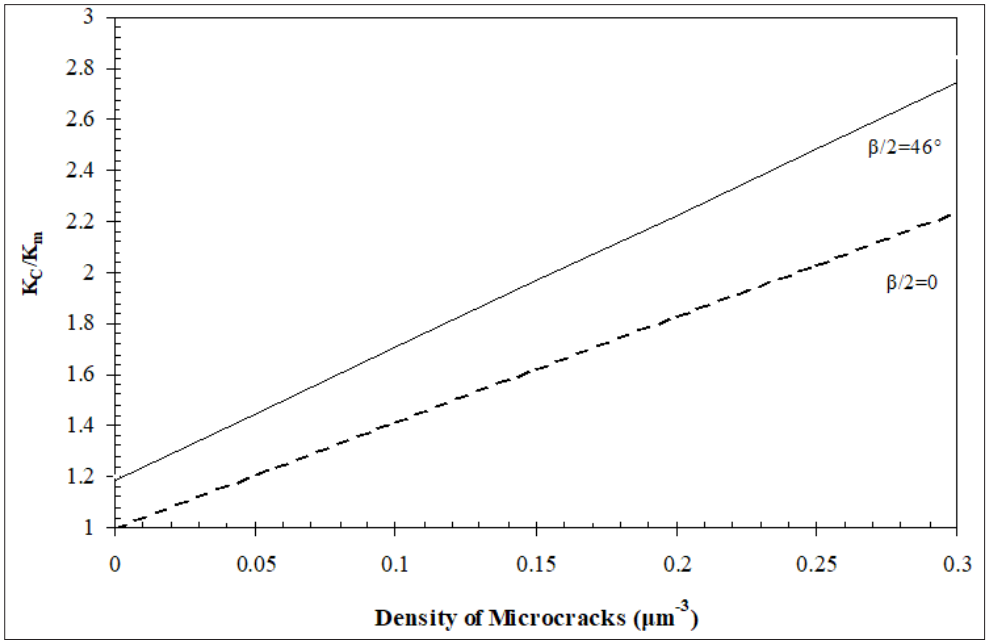

Figure 7: Fracture toughness increases in a linear fashion with increasing microcrack density based on the branching and microcracking model proposed by Gao & Wang [37] (p/a=0.25).

Replacing the Gao and Wang's model [37] the fracture toughness of the 3 wt% nanoclay-filled epoxy (KIC=1.1MPam0.5) and the neat epoxy (KIC=0.8MPam0.5) and, back calculating predicts a 116° angle (β/2=58°) as the angle of the branched crack if the density of the microcracks is assumed equal to zero. The angle of branched crack was measured about 92° (β/2=46°) for the 3 wt% intercalated clay-epoxy system from (Figure 4b). Assuming no secondary microcracking and substituting the angle of branched crack equal to 92° (β/2=46°) in the model proposed by Gao & Wang [37] estimates a 20% increase in fracture toughness compared to a 37% increase observed in the experiment. This difference suggests that for the 3 wt% intercalated clay-epoxy, a part of the improvements in toughness can be due to the crack branching, which acts as a shielding micro mechanism and possibly further increases the toughness by microcracking since there is the evidence of secondary microcracking in the TOM micrograph (Figure 4c). (Figure 7) depicts linear increases in the overall fracture toughness as a function of microcracks density. Microcracking has

been observed as a major toughening mechanism in hollow glass spheres-filled and thermoplastic-modified epoxies [41,42] under both static and cyclic loading conditions. More data points are needed to investigate the toughening contribution of branching and microcracking in a systematic approach as a function of filler content. The present study cannot definitely answer whether the branching angle is a function of the filler concentration and if the branching and microcracking can be a major source of energy dissipation in a range of formulations. Based on the experimental results and available micromechanical models, it might be concluded that at lower contents of organoclay, crack branching and microcracking are the major sources of toughening rather than crack path deflection, while crack path deflection is dominant at higher contents of filler due to morphology aspects. In addition, the present study proposes the possible additive effects of crack path deflection, crack wake bridging, and crack branching and microcracking as the source of modest improvements in toughness for intercalated clay-filled epoxies. The supplemental studies need to clarify these aspects.

Summary and Conclusions

The results of this work may be summarized as follows: Both TEM and XRD revealed that the organoclay was intercalated and that the spacing between platelets was about 3.5nm. The incorporation of intercalated organoclay did not change the glass transition temperature of the epoxy resin. Therefore, the incorporation of nanoclay into a ductile epoxy resin does not interfere with the cure reaction and the surfactant does not significantly plasticize the epoxy used in this study. The fracture toughness is increased with incorporation of intercalated nanoclay. The nanocomposite containing 5 wt% nanoclay exhibited the highest toughness; however, a 50% increase in fracture toughness is modest when compared to other filled epoxies. The modest increase in fracture toughness agrees with numerous studies in the literature and suggests that these types of fillers are not very effective toughening agents. Scanning electron microscopy (SEM) and transmission optical microscopy (TOM) revealed that the improvements in fracture toughness can be attributed to crack deflection, crack branching and microcracking in these intercalated clay-filled epoxy nanocomposites. In addition, the predicted values using micromechanical models suggested crack branching/microcracking as the effective toughening mechanism in these materials.

References

1. Carolan D, Ivankovic A, Kinloch AJ, Sprenger S, Taylor AC (2016) Toughening of epoxy-based hybrid nanocomposites. Polymer 97: 179-190.
2. Vijayan PP, Puglia D, Al Maadeed MASA, Kenny JM, Thomas S (2017) Elastomer/thermoplastic modified epoxy nanocomposites: The hybrid effect of micro and nano scale. Materials Science and Engineering: R: Reports 116: 1-29.
3. Kamar NT, Drzal LT (2016) Micron and nanostructured rubber toughened epoxy: A direct comparison of mechanical, thermomechanical and fracture properties. Polymer 92: 114-124.
4. Bakis G, Kothmann MH, Zeiler R, Brückner A, Ziadeh M, et al. (2018) Influence of size, aspect ratio and shear stiffness of nanoclays on the fatigue crack propagation behavior of their epoxy nanocomposites. Polymer 158: 372-380.
5. Hmeidat NS, Kemp JW, Compton BG (2018) High-strength epoxy nanocomposites for 3D printing. Composites Science and Technology 160: 9-20.
6. Moloney AC, Kausch HH, Kaiser T, Beer HR (1987) Parameters determining the strength and toughness of particulate filled epoxide resins. Journal of Materials Science 22: 381-393.
7. Marouf BT, Mai YW, Bagheri R, Pearson RA (2016) Toughening of epoxy nanocomposites: Nano and hybrid effects. Polymer Reviews 56(1): 70-112.
8. Argon AS, Cohen RE (2003) Toughenability of polymers. Polymer 44(19): 6013-6032.
9. Bagheri R, Marouf BT, Pearson RA (2009) Rubber-toughened epoxies: A critical review. Polymer Reviews 49(3): 201-225.
10. Kinloch AJ, Taylor AC (2003) Mechanical and fracture properties of epoxy/inorganic micro- and nano-composites. Journal of Materials Science Letters 22: 1439-1441.
11. Azeez AA, Rhee KY, Park SJ, Hui D (2013) Epoxy clay nanocomposites-processing, properties and applications: A review. Composites Part B: Engineering 45(1): 308-320.
12. Marouf BT, Pearson RA, Bagheri R (2017) Modeling of stiffening and strengthening in nano-layered silicate/epoxy. International Journal of Engineering 30(1): 93-100.
13. Marouf BT, Pearson RA, Bagheri R (2009) Anomalous fracture behavior in an epoxy-based hybrid composite. Materials Science and Engineering: A 515(1-2): 49-58.
14. Paul DR, Robeson LM (2008) Polymer nanotechnology: Nanocomposites. Polymer 49(15): 3187-3204.
15. Luo JJ, Daniel IM (2003) Characterization and modeling of mechanical behavior of polymer/clay nanocomposites. Composites Science and Technology 63(11): 1607-1616.
16. Fornes TD, Paul DR (2003) Modeling properties of nylon 6/clay nanocomposites using composite theories. Polymer 44(17): 4993-5013.
17. Rafiee R, Shahzadi R (2018) Predicting mechanical properties of nanoclay/polymer composites using stochastic approach. Composites Part B: Engineering 152: 31-42.
18. Százdi L, Pukánszky B, Vancso GJ, Pukánszky B (2006) Quantitative estimation of the reinforcing effect of layered silicates in PP nanocomposites. Polymer 47(13): 4638-4648.
19. Százdi L, Pozsgay A, Pukánszky B (2007) Factors and processes influencing the reinforcing effect of layered silicates in polymer nanocomposites. European Polymer Journal 43(2): 345-359.
20. Brunner AJ, Necola A, Rees M, Gasser P, Kornmann X, et al. (2006) The influence of silicate-based nano-filler on the fracture toughness of epoxy resin. Engineering Fracture Mechanics 73(16): 2336-2345.
21. Qi B, Zhang QX, Bannister M, Mai YW (2006) Investigation of the mechanical properties of DGEBA-based epoxy resin with nanoclay additives. Composite Structures 75(1-4): 514-519.
22. Miyagawa H, Drzal LT (2004) The effect of chemical modification on the fracture toughness of montmorillonite clay/epoxy nanocomposites. Journal of Adhesion Science and Technology 18(13): 1571-1588.
23. Koh KL, Ji X, Dasari A, Lu X, Lau SK, et al. (2017) Fracture toughness and elastic modulus of epoxy-based nanocomposites with dopamine-modified nano-fillers. Materials 10(7): 776.

24. Zerda AS, Lesser AJ (2001) Intercalated clay nanocomposites: Morphology, mechanics, and fracture behavior. Journal of Polymer Science Part B: Polymer Physics 39(11): 1137-1146.

25. Zilg C, Mülhaupt R, Finter J (1999) Morphology and toughness/stiffness balance of nanocomposites based upon anhydride-cured epoxy resins and layered silicates. Macromolecular Chemistry and Physics 200(3): 661-670.

26. Kinloch AJ, Taylor AC (2006) The mechanical properties and fracture behaviour of epoxy-inorganic micro- and nano-composites. Journal of Materials Science 41: 3271-3297.

27. Wang K, Chen L, Wu J, Toh ML, He C, et al. (2005) Epoxy nanocomposites with highly exfoliated clay: Mechanical properties and fracture mechanisms. Macromolecules 38(3): 788-800.

28. Kraus G, Gruver JT (1970) Thermal expansion, free volume, and molecular mobility in a carbon black-filled elastomer. Journal of Polymer Science Part A-2: Polymer Physics 8(4): 571-581.

29. Liu W, Hoa SV, Pugh M (2005) Organoclay-modified high performance epoxy nanocomposites. Composites Science and Technology 65(2): 307-316.

30. Killi K, Srikanth I, Rangababu B, Majee SK, Bauri R, et al. (2015) Effect of nanoclay on the toughness of epoxy and mechanical, impact properties of e-glass-epoxy composites. Advanced Materials Letter 6(6): 684.

31. Zappalorto M, Salviato M, Quaresimin M (2013) Mixed mode (I+II) fracture toughness of polymer nanoclay nanocomposites. Engineering Fracture Mechanics 111: 50-64.

32. Atif R, Inam F (2016) Fractography analysis of 1.0 wt% nanoclay/multi-layer graphene reinforced epoxy nanocomposites. Journal of Composite Materials 51(23): 3281-3290.

33. Varano E, Zhou M, Lanham S, Iredale RJ, Duijneveldt JS, et al. (2019) Developing toughened bismaleimide-clay nanocomposites: Comparing the use of platelet and rod-like nanoclays. Reactive and Functional Polymers 134: 10-21.

34. Suresh S, Shih CF (1986) Plastic near-tip fields for branched cracks. International Journal of Fracture 30: 237-259.

35. Faber KT, Evans AG (1983) Crack deflection processes-I Theory. Acta Metallurgica 31(4): 565-576.

36. Hutchinson JW (1987) Crack tip shielding by micro-cracking in brittle solids. Acta Metallurgica 35(7): 1605-1619.

37. Gao F, Wang T (1990) Apparent fracture energy of brittle materials by branching of crack and microcrack. Journal of Materials Science Letters 9: 1409-1411.

38. Evans AG, Fu Y (1985) Some effects of microcracks on the mechanical properties of brittle solids-II. Microcrack toughening. Acta Metallurgica 33(8): 1525-1531.

39. Ortiz M (1987) A continuum theory of crack shielding in ceramics. Journal of Applied Mechanics 54(1): 54-58.

40. Evans AG, Faber KT (1981) Toughening of ceramics by circumferential microcracking. Journal of the American Ceramic Society 64(7): 394-398.

41. Pearson RA, Yee AF (1993) Toughening mechanisms in thermoplastic-modified epoxies: 1. Modification using poly(phenylene oxide). Polymer 34(17): 3658-3670.

42. Azimi HR, Pearson RA, Hertzberg RW (1996) Fatigue of hybrid epoxy composites: Epoxies containing rubber and hollow glass spheres. Polymer Engineering & Science 36(18): 2352-2365.